

Article

Mechanical Dispersion of Nanoparticles and Its Effect on the Specific Heat Capacity of Impure Binary Nitrate Salt Mixtures

Mathieu Lasfargues ¹, Qiao Geng ², Hui Cao ² and Yulong Ding ^{2,*}

¹ School of Chemical and Process Engineering, University of Leeds, Leeds LS2 9JT, UK;
E-Mail: m.lasfargues@leeds.ac.uk

² School of Chemical Engineering, University of Birmingham, Birmingham B15 2TT, UK;
E-Mails: gxq471@student.bham.ac.uk (Q.G.); h.cao@bham.ac.uk (H.G.)

* Author to whom correspondence should be addressed; E-Mail: y.ding@bham.ac.uk;
Tel.: +44-121-414-5297.

Academic Editor: Jiye Fang

Received: 25 May 2015 / Accepted: 19 June 2015 / Published: 29 June 2015

Abstract: In this study, the effect of nanoparticle concentration was tested for both CuO and TiO₂ in eutectic mixture of sodium and potassium nitrate. Results showed an enhancement in specific heat capacity (C_p) for both types of nanoparticles (+10.48% at 440 °C for 0.1 wt % CuO and +4.95% at 440 °C for 0.5 wt % TiO₂) but the behavior toward a rise in concentration was different with CuO displaying its highest enhancement at the lowest concentration whilst TiO₂ showed no concentration dependence for three of the four different concentrations tested. The production of cluster of nanoparticles was visible in CuO but not in TiO₂. This formation of nanostructure in molten salt might promote the enhancement in C_p . However, the size and shape of these structures will most likely impact the energy density of the molten salt.

Keywords: nanoparticles; molten salt; energy storage

1. Introduction

The addition of nanoparticles into a base liquid forms a two-phase mixture termed nanofluid by Choi in 1995 [1]. With nominal size ranging from 1 to 100 nm, these nanoparticles have been reported to display anomalous enhancement of the thermal characteristics of the fluid within which they are suspended. The addition of varied fraction of nanoparticles (Al₂O₃, Au, Cu, TiO₂, CuO, carbon

nanotube...) into base fluid such as pumped oil, glycerol, toluene, water have shown enhanced thermal conductivity with minutes addition (maximum of 5.0 vol. %) [2–11]. The multifaceted nature of nanofluids has been difficult to model and reported data have shown that various factors such as size of particle, concentration, particle surface properties, shape, interaction between base liquid and particle could affect the thermal characteristics in different manners [3,8,12–20]. With the literatures been full of papers reporting these abnormal enhancements in thermal conductivity, recent theory and understanding points toward the effective medium theory by Maxwell as a good model for the prediction of thermal conductivity [21,22]. However, very little experiments in comparison have been conducted on heat capacity and modelling of non-ionic fluids using classical and statistical model has shown good agreement with the obtained data following the equation below [23]:

$$C_{p,nf} = \frac{\phi(\rho C_p)_n + (1 - \phi)(\rho C_p)_f}{\phi \rho_n + (1 - \phi)\rho_f}$$

where C_p , ϕ , ρ , nf , n and f respectively represent specific heat capacity, volume fraction, density, nanofluid, nanoparticle and fluid. It has implied that increased thermal conductivity has been translated into decrease in specific heat capacity as shown by Pantzali *et al.* [24]. However this has not been the case in ionic fluids such as molten salt where the addition of nanoparticles into this liquid base has promoted an enhancement in specific heat capacity which does not follow the above equation. Indeed various publications have demonstrated a general rise in specific heat capacity when nanoparticles were added to the system [25–31]. This paper looks at the effect of various concentrations (0.1 wt % to 1.5 wt %) of copper oxide and titanium dioxide on the specific heat capacity, as well as the enthalpy of melting.

2. Experimental Section

2.1. Salt Production and Nanoparticles Dispersion

Sodium nitrate (FISHER, Loughborough, UK) (98% Pure) and potassium nitrate (SIGMA-ALDRICH, Suffolk, UK) (98% Pure) were purchased for these tests. Using a Ball-Mill Model (Pascall Engineering, Sussex, UK; BERCO, S/N 17520) with 9 mm stainless steel bearing, the eutectic mixture was grinded and mixed with the following ratio of salts (60 wt % NaNO_3 + 40 wt % KNO_3), melted at 300 °C for a few hours before been grinded again into fine powder. The purity of the sample was intentionally low to ensure it met similar criteria to that used in a concentrated solar power plant where it would not be economically viable to utilise high purity salt mixture.

Oxide nanoparticles of copper (QinetiQ Nanomaterials Limited, Farnborough, UK) and titanium (Nanophase NanoTek, Romeoville, IL, USA) with APS size of 29 nm and 34 nm respectively were dispersed into the binary mixture of nitrate using ball-mill with 9 mm stainless steel bearing.

Unlike other papers, the methodology does not involve the use of water to dissolve the salt and disperse the nanoparticle through sonication before re-crystallisation, drying and eventually melting is to take place. Even when using such methods, it has been showed that agglomeration of nanoparticles occurs. Here the dispersion is purely physical through the use of a ball-mill.

2.2. Differential Scanning Calorimeter (DSC)

Specific heat capacity (C_p) and enthalpy of change were measured using heat-flux differential scanning calorimeter (DSC) with automated sampler (DSC 1, Mettler Toledo, Leicester, UK). The C_p measurements were carried out through a standard procedure using a sapphire reference. The thermal cycle started with a 5 min isothermal at 250 °C followed by a dynamic phase with a ramp rate of 40 °C/min to 450 °C and another 5 min isothermal at 450 °C. Three samples were produced for each blend and each sample was consecutively tested three times.

Specific heat capacity was first calculated for sapphire in order to check the validity of the methodology. With variation obtained of the order of $\pm 0.3\%$ compared to that of the reference values, the approach was deemed accurate enough to start the tests on both CuO and TiO₂ doped salt.

The samples were then loaded into 30 μ L platinum crucibles (Mettler Toledo). The latter were placed onto a hot-plate and heated up to 250 °C for 30 min to allow the salt to melt before been loaded onto the carousel ready for testing.

2.3. Scanning Electron Microscopy (SEM) and Energy Dispersive X-Ray (EDX)

Morphological analysis of the samples was carried out using a field emission scanning electron microscopy Hitachi SU8230 (Hitachi, Berkshire, UK). Samples were mounted after DSC measurements on 12 mm diameter aluminium scanning electron microscopy (SEM) stub and coated with 3 nm of platinum/palladium mixture (80/20 Ratio) using a high resolution sputter coater.

3. Results and Discussions

The use of copper oxide revealed a concentration dependency where the lowest ratio (0.1 wt %) promoted the highest rise in C_p (10.48% at 440 °C—Table 1) with a decrease seen as the amount added rose to 1.5 wt % (Figure 1A). This was also indicated in Table 1 where the percentage enhancement in C_p decreases with a rise the concentration of CuO (10.48% for 0.1 wt %, 9.18% for 0.5 wt %, 8.49% for 1.0 wt % and 2.19% for 1.5 wt % CuO at 440 °C, see Table 1). The latter showed a detrimental behavior to the specific heat capacity (Figure 1A, Table 1—CuO). This has been reported by Chieruzzi *et al.* which showed negative enhancement when using 0.5 and 1.5 wt % SiO₂ whilst 1.0 wt % SiO₂ provided increase in C_p indicating the need for an optimum ratio [32,33]. Unlike Chieruzzi's research, test on TiO₂ (Figure 1B) led to a similar rise in C_p with 0.5, 1.0 and 1.5 wt % of TiO₂ achieving a 5.0% increase at 440 °C (Table 1—TiO₂) [32]. Presumably the different methodology in the dispersion of nanoparticles as well as size and production process of the nanoparticle itself would account for these differing results obtained.

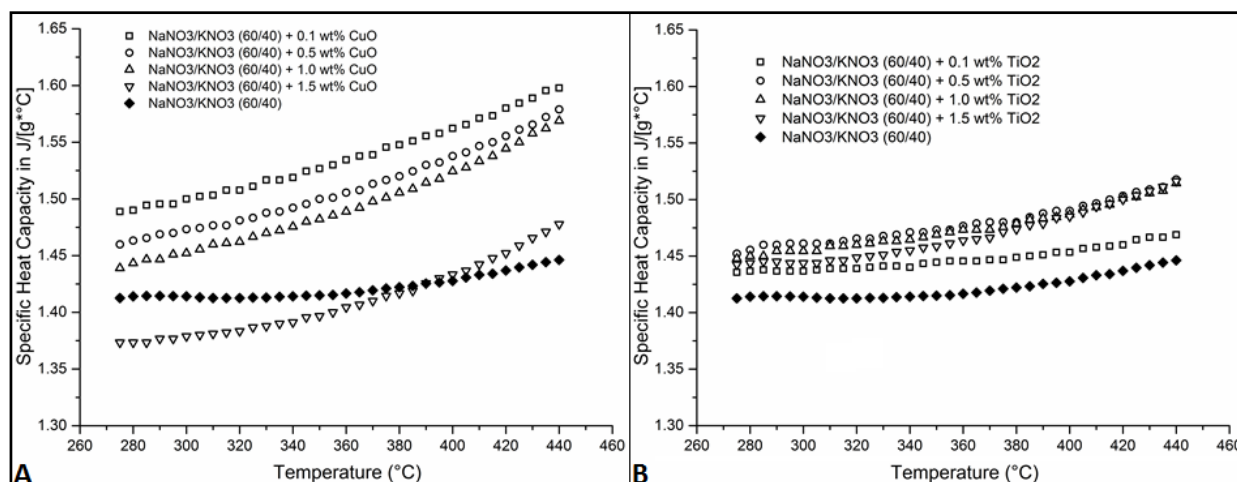


Figure 1. Specific heat capacity (C_p) measurements: (A) 0.1 to 1.5 wt % CuO addition to 60/40 mixtures of Na/K-NO₃; (B) 0.1 to 1.5 wt % TiO₂ addition to 60/40 mixtures of Na/K-NO₃.

Table 1. Percentage increase in specific heat capacity (C_p) compared to base salt for different concentrations of CuO and TiO₂.

Temperature °C	0.1 wt % CuO	0.5 wt % CuO	1.0 wt % CuO	1.5 wt % CuO	0.1 wt % TiO ₂	0.5 wt % TiO ₂	1.0 wt % TiO ₂	1.5 wt % TiO ₂
	% Increase	% Increase	% Increase	% Increase				
265	4.87	2.97	1.47	-2.79	1.39	2.66	2.03	2.07
300	6.08	4.19	2.70	-2.49	1.60	3.33	2.86	2.10
350	7.90	6.02	4.76	-1.29	2.09	4.13	3.82	3.10
400	9.43	7.71	6.78	0.40	1.80	4.37	4.13	4.02
440	10.48	9.18	8.49	2.19	1.57	4.95	4.72	4.85

The trend in the average heat of fusion of copper oxides decreases from 99.99 J/g with 0.1 wt % to 89.84 J/g with 1.5 wt %. The heat of fusion of 0.5, 1.0 and 1.5 wt % of TiO₂ is very similar at ≈98.00 J/g when 0.1 wt % displays 101.31 J/g. It is not surprising to see such trend showing up as the dispersion of nanoparticles and the presence/size of agglomerate will affect both of these characteristics by altering the entropy of the medium. Whilst trend can be spotted, the relationship is still a difficult one to understand and it seems that large enhancement in the heat of fusion could forecast a high C_p increase albeit the result from 0.1 wt % TiO₂ goes against this statement. However the largest enhancements in enthalpy seen in Chieruzzi *et al.* were also the one where the rises in C_p were the highest [32]. The formation of nano-structures whereby salt would be trapped inside tiny agglomerates could help understand this rise in enthalpy as more energy would be required to melt the solid trapped within these structures. The presence of nanoparticles (CuO and TiO₂) within the molten salt would also lead to a broader melting range with a slight increase in the melting point. This is the case for TiO₂ curves (small Table in Figure 3) but CuO does not fit this trend. Indeed for copper oxide, the melting point decrease from 223.86 °C for 0.1 wt % of CuO to 221.26 °C for 0.5 wt % and 220.66 °C when 1.0 wt % is utilized and then the melting point is back up to 224.12 °C at 1.5 wt % (small Table in Figure 2). This could be explained by a change in the amount and size of aggregate present as well

as the way heat is transferred via nanoparticles (Diffuse or Ballistic) as the concentration of copper oxide rises from 0.1 wt % to 1.5 wt %.

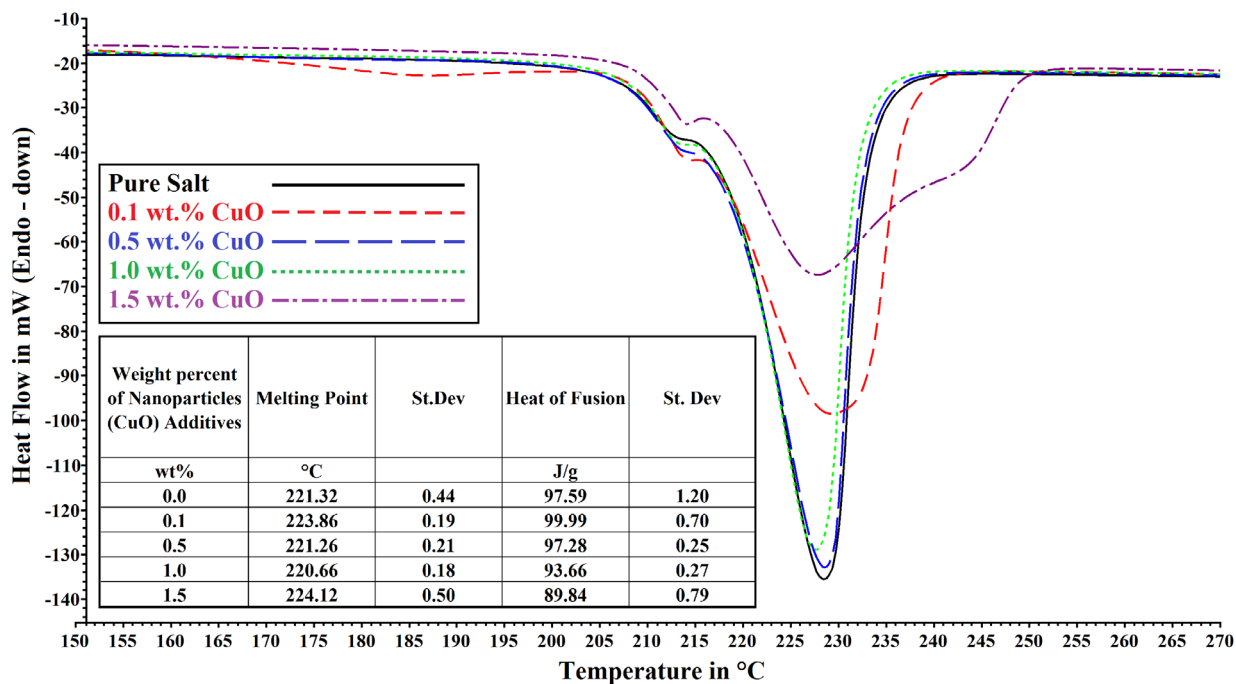


Figure 2. Differential scanning calorimetry (DSC) curves of NaNO₃ and KNO₃ eutectic mixture (60/40) with and without CuO nanoparticles. Table inserted in the graph shows the average melting point and heat of fusion values.

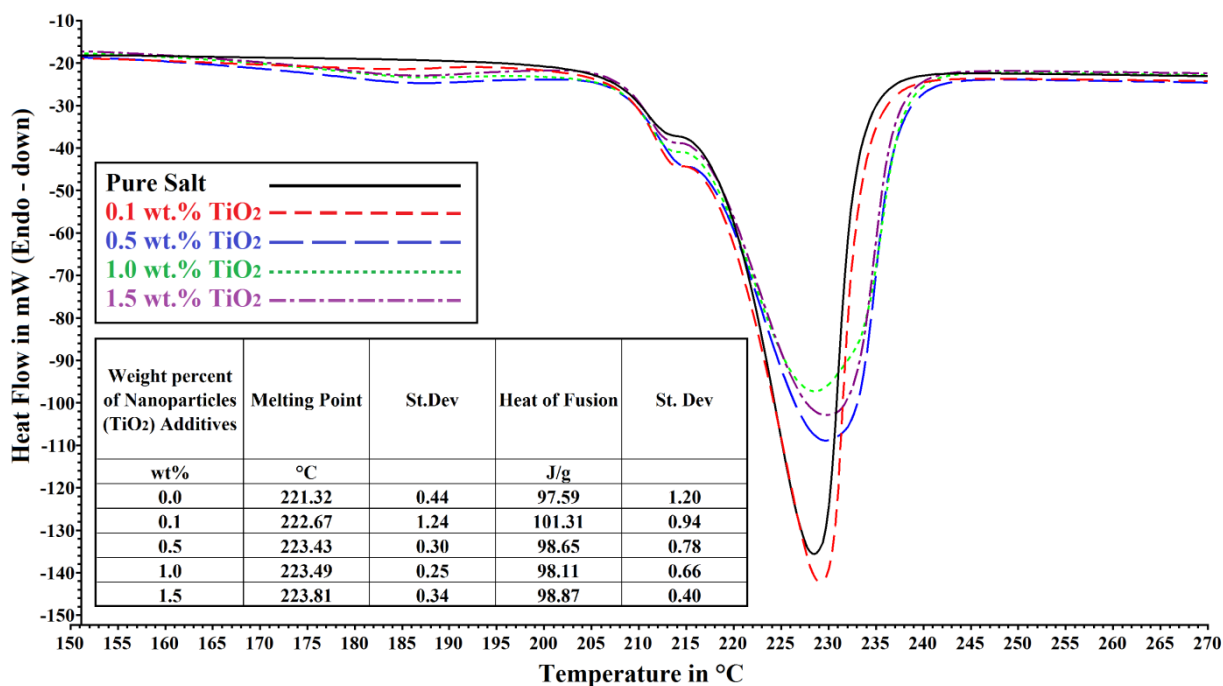


Figure 3. DSC curves of NaNO₃ and KNO₃ eutectic mixture (60/40) with and without TiO₂ nanoparticles. Table inserted in the graph shows the average melting point and heat of fusion values.

The dispersion of the nanoparticles was heterogeneous with large agglomerates seen both on the EDX mapping and on the SEM images. Various scanned spectrums showed that some areas were devoid of nanoparticles (Spectrums 6 and 8 on Figure 4, Spectrum 3 on Figure 5) whilst other showed large structure which looked to be interconnected with each other (Figures 4 and 5—EDX Mapping—Yellow and Violet). Similarly the SEM images clearly show that some areas of the molten salt are free from nanoparticles (Blue arrow on Figures 6 and 7) with other portions filled with big interconnected nanoparticles structures (Red circle on Figure 6). Lu and Huang, 2013 made the same observation with agglomeration of nanoparticles been easily distinguishable when Al_2O_3 was present ²⁵. This was also showed and confirmed by Shin 2011 for SiO_2 [28].

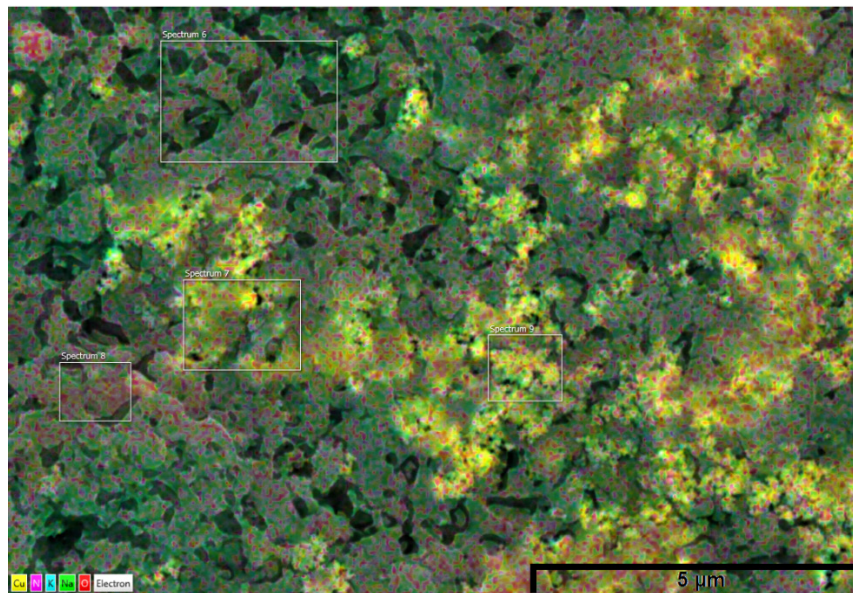


Figure 4. Energy dispersive X-ray (EDX) mapping of 0.1 wt % CuO (Yellow—Copper, Violet—Nitrogen, Blue—Potassium, Green—Sodium, and Red—Oxygen).

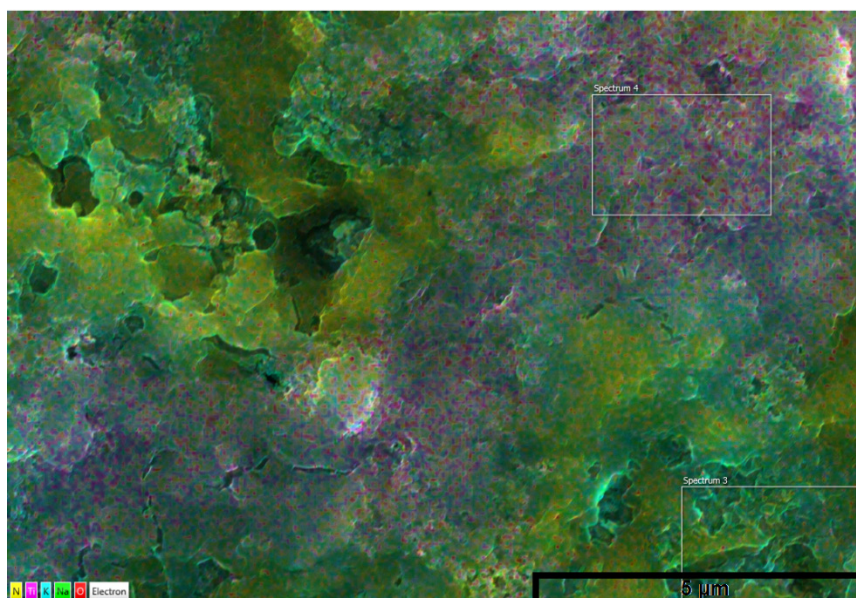


Figure 5. EDX mapping of 0.1 wt % TiO₂ (Yellow—Nitrogen, Violet—Titanium, Blue—Potassium, Green—Sodium, and Red—Oxygen).

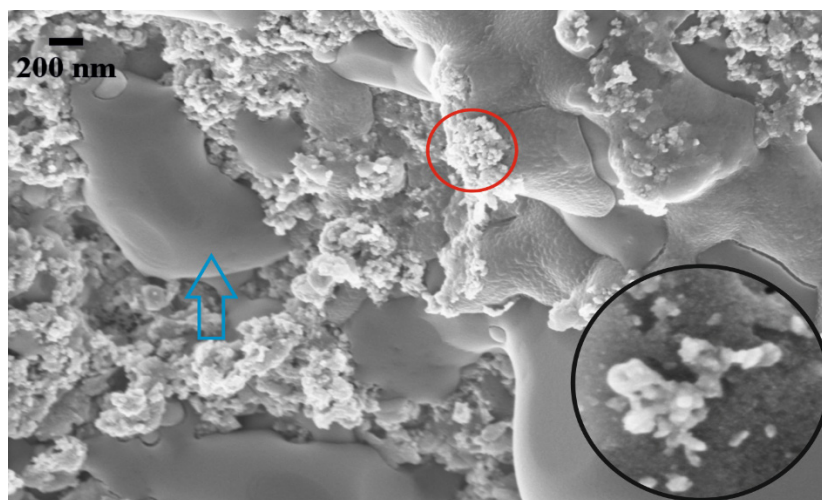


Figure 6. Scanning electron microscopy (SEM) image of 1.0 wt % Copper Oxide ($\times 75,000$ magnification). The blue arrow points at the surface of molten salt free from nanoparticles whilst the red circle shows agglomerate of CuO. Bottom right side shows a magnified image of copper oxide nanoparticles.

In this study both EDX and SEM clearly show agglomerated nanoparticles, which are similar to other publications [25,29,30,33,34]. Whilst it is possible to have well dispersed nanoparticles in liquid phase, the most likely scenario is the production of agglomerates within molten salt. The latter depending on their size will affect the energy density. Furthermore the shape of the nanoparticles is likely to affect the volume of nano-layers surrounding the particles. The TiO_2 particles were spherical in shape with heterogeneous size distribution (Figure 7), whilst the CuO seemed to display a heterogeneous shape distribution whilst their size appeared to be more evenly distributed (Figure 6). The latter (Figure 6) displayed clusters of agglomerate unlike the TiO_2 which seemed to show an interconnected layer of nanoparticles as shown on Figure 7. Could the production of small agglomerates be helpful toward the enhancement of C_p ? If that is so, then this variable would be a key factor in the definition of C_p .

Furthermore, other variables such as loading factor, shape, size, density, homogeneity, surface charge and type will affect its behaviour in molten salt. With less than 20 published articles investigating this phenomenon, not enough data is available to try and devise a good model as to why this anomalous rise is observed.

In its liquid phase it is hypothesised that the enhancement in specific heat capacity comes from the interaction between the ionic liquid and the solid nanoparticles through the production of nano-layers. The latter would occur at the interface between the ionic liquid and the solid nanoparticle's surface where the former behave as a semi-solid due to constraints surrounding the atoms. Because the enhancement in specific heat capacity cannot come from the nanoparticles themselves as the latter display lower values than the salt [35], the increase in C_p could be explained by partially incorporating the enthalpy of fusion in this loosely parked semi-solid structure [31]. The production of structured layers at an interface with a solid has been observed Oh *et al.* research team where their research showed that liquid aluminium atoms at the interface with sapphire were constrained into layers [36].

A further two other modes might affect this anomalous enhancement in C_p . First, the higher C_p of nanoparticles themselves (compared to bulk) which has been reported by Tan *et al.* whereby the small particle size leads to the increased exposure of surface atoms [35]. The latter are less constrained and possess an excess volume in comparison to the atoms within its centre which as demonstrated by Wang *et al.* led to a blue shift in wave number for Al_2O_3 nanoparticles compared to bulk confirming this hypothesis [37]. Finally the interfacial thermal resistance could also have an impact on the enhancement of specific heat capacity due to an increase surface area to volume ratio provided by the nanoparticles if the latter are well dispersed. Whilst these three modes might each play a role in the enhancement of C_p , it is believed that the formation of nano-layers would be the main driving force toward the anomalous rise in C_p observed.

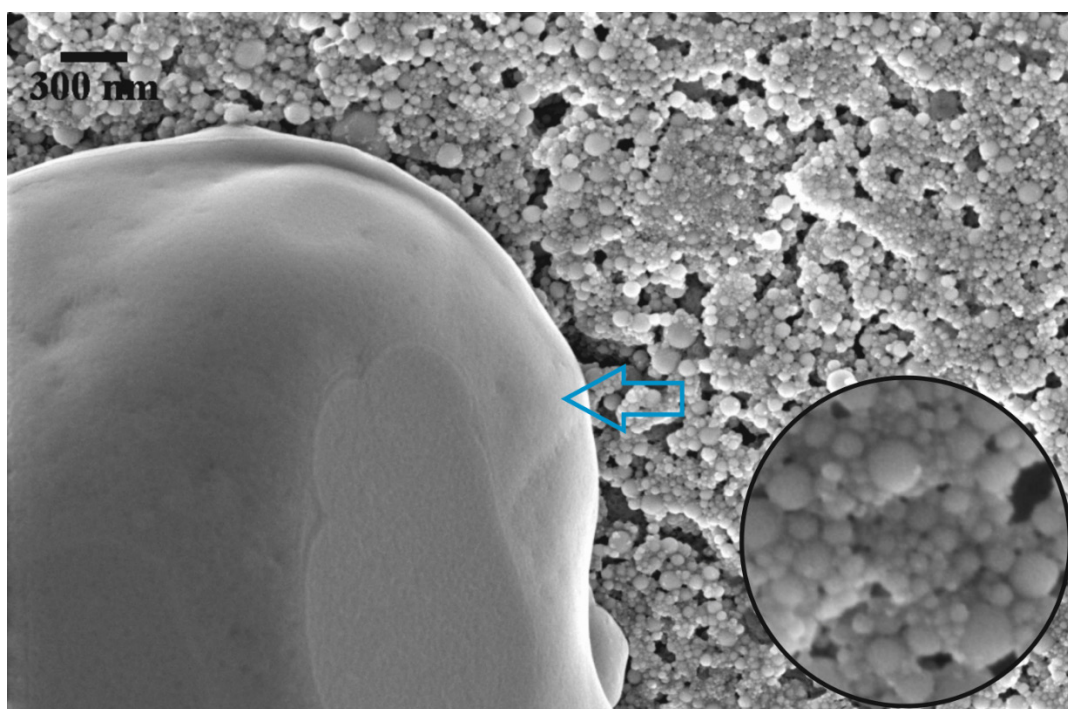


Figure 7. SEM image of 1.0 wt % TiO_2 ($\times 75,000$ magnification). The blue arrow points at the surface of molten salt free from nanoparticles. Bottom right side shows a magnified image of titanium dioxide nanoparticles.

4. Conclusions

In this study, we investigated the dispersion of two types of nanoparticles in molten salt mixture (60 wt % NaNO_3 and 40 wt % KNO_3). The results showed that the variation in C_p was dependent on the concentration for CuO (Table 1). However TiO_2 behaved in a different manner showing no dependence on concentration with 0.5, 1.0 and 1.5 wt % concentration displaying similar enhancement in C_p (Table 1). Furthermore the SEM data showed the production of clusters of nano-particle when CuO was present. This was not the case for TiO_2 which showed a large interconnected layer rather than cluster. The shape and size distribution of the nanoparticles were very different which would impact its behaviour in the liquid phase. It is thought that the production of small agglomerates/nanostructures could have a beneficial impact on the enhancement of C_p .

The development of heat-transfer-fluid in concentrated solar power plant application is an important field of research, as any enhancement in specific heat capacity would directly impact the storage capacity and price of production. As molten salt are one of the best alternative to synthetic oil, understanding how nanoparticles behave in such liquid might lead to the development of a more thermodynamically efficient HTF.

Acknowledgment

Financial support was provided by EPSRC EP/L014211/1 (Next generation grid scale thermal energy storage technologies), and EPSRC EP/K002252/1.

Author Contributions

All authors contributed extensively to the work presented in this paper.

Conflicts of Interest

The authors declare no conflict of interest.

References

1. Choi, S.U.S.; Eastman, J.A. Enhancing Thermal Conductivity of Fluids with Nano-Particles. In Proceedings of the International Mechanical Engineering Congress and Exposition, San Francisco, CA, USA, 12–17 November 1995.
2. Lee, S.; Choi, S.U.S.; Li, S.; Eastman, J.A. Measuring thermal conductivity of fluids containing oxide nanoparticles. *J. Heat Transf.-Trans. Asme* **1999**, *121*, 280–289.
3. Das, S.K.; Putra, N.; Thiesen, P.; Roetzel, W. Temperature dependence of thermal conductivity enhancement for nanofluids. *J. Heat Transf.-Trans. Asme* **2003**, *125*, 567–574.
4. Patel, H.E.; Das, S.K.; Sundararajan, T.; Nair, A.S.; George, B.; Pradeep, T. Thermal conductivities of naked and monolayer protected metal nanoparticle based nanofluids: Manifestation of anomalous enhancement and chemical effects. *Appl. Phys. Lett.* **2003**, *83*, 2931–2933.
5. Wen, D.S.; Ding, Y.L. Experimental investigation into convective heat transfer of nanofluids at the entrance region under laminar flow conditions. *Int. J. Heat Mass Transf.* **2004**, *47*, 5181–5188.
6. Wen, D.S.; Ding, Y.L. Formulation of nanofluids for natural convective heat transfer applications. *Int. J. Heat Fluid Flow* **2005**, *26*, 855–864.
7. Xie, H.Q.; Wang, J.C.; Xi, T.G.; Liu, Y.; Ai, F. Dependence of the thermal conductivity of nanoparticle-fluid mixture on the base fluid. *J. Mater. Sci. Lett.* **2002**, *21*, 1469–1471.
8. Zhang, X.; Gu, H.; Fujii, M. Effective thermal conductivity and thermal diffusivity of nanofluids containing spherical and cylindrical nanoparticles. *Exp. Therm. Fluid Sci.* **2007**, *31*, 593–599.
9. Eastman, J.A.; Choi, S.U.S.; Li, S.; Yu, W.; Thompson, L.J. Anomalous increased effective thermal conductivities of ethylene glycol-based nanofluids containing copper nanoparticles. *Appl. Phys. Lett.* **2001**, *78*, 718–720.

10. He, Y.; Jin, Y.; Chen, H.; Ding, Y.; Cang, D.; Lu, H. Heat transfer and flow behaviour of aqueous suspensions of TiO₂ nanoparticles (nanofluids) flowing upward through a vertical pipe. *Int. J. Heat Mass Transf.* **2007**, *50*, 2272–2281.
11. Ding, Y.L.; Alias, H.; Wen, D.S.; Williams, R.A. Heat transfer of aqueous suspensions of carbon nanotubes (CNT nanofluids). *Int. J. Heat Mass Transf.* **2006**, *49*, 240–250.
12. Ding, Y.L.; Chen, H.; Wang, L.; Yang, C.-Y.; He, Y.; Yang, W.; Lee, W.P.; Zhang, L.; Huo, R. Heat transfer intensification using nanofluids. *Kona-Powder Part.* **2007**, *25*, 23–38.
13. Xie, H.Q.; Wang, J.; Xi, T.; Liu, Y.; Ai, F.; Wu, Q. Thermal conductivity enhancement of suspensions containing nanosized alumina particles. *J. Appl. Phys.* **2002**, *91*, 4568–4572.
14. Trisaksri, V.; Wongwises, S. Critical review of heat transfer characteristics of nanofluids. *Renew. Sustain. Energy Rev.* **2007**, *11*, 512–523.
15. Yu, W.; Xie, H. A review on nanofluids: Preparation, stability mechanisms, and applications. *J. Nanomater.* **2012**, *2012*, doi:10.1155/2012/435873.
16. Yang, X.; Liu, Z. A kind of nanofluid consisting of surface-functionalized nanoparticles. *Nanoscale Res. Lett.* **2010**, *5*, 1324–1328.
17. Prasher, R.; Phelan, P.E.; Bhattacharya, P. Effect of aggregation kinetics on the thermal conductivity of nanoscale colloidal solutions (nanofluid). *Nano Lett.* **2006**, *6*, 1529–1534.
18. Lee, D.; Kim, J.W.; Kim, B.G. A new parameter to control heat transport in nanofluids: Surface charge state of the particle in suspension. *J. Phys. Chem. B* **2006**, *110*, 4323–4328.
19. Das, S.K.; Choi, S.U.S.; Patel, H.E. Heat transfer in nanofluids—A review. *Heat Transf. Eng.* **2006**, *27*, 3–19.
20. Xuan, Y.M.; Li, Q. Heat transfer enhancement of nanofluids. *Int. J. Heat Fluid Flow* **2000**, *21*, 58–64.
21. Koblinski, P.; Prasher, R.; Eapen, J. Thermal conductance of nanofluids: Is the controversy over? *J. Nanoparticle Res.* **2008**, *10*, 1089–1097.
22. Buongiorno, J.; Venerus, D.C.; Prabhat, N.; McKrell, T.; Townsend, J.; Christianson, R.; Tolmachev, Y.V.; Koblinski, P.; Hu, L.-W.; Alvarado, J.L.; *et al.* A benchmark study on the thermal conductivity of nanofluids. *J. Appl. Phys.* **2009**, *106*, doi:10.1063/1.3245330.
23. Zhou, S.-Q.; Ni, R. Measurement of the specific heat capacity of water-based Al(2)O(3) nanofluid. *Appl. Phys. Lett.* **2008**, *92*, doi:10.1063/1.2890431.
24. Pantzali, M.N.; Kanaris, A.G.; Antoniadis, K.D.; Mouza, A.A.; Paras, S.V. Effect of nanofluids on the performance of a miniature plate heat exchanger with modulated surface. *Int. J. Heat Fluid Flow* **2009**, *30*, 691–699.
25. Lu, M.C.; Huang, C.H. Specific heat capacity of molten salt-based alumina nanofluid. *Nanoscale Res. Lett.* **2013**, *8*, doi:10.1186/1556-276x-8-292.
26. Shin, D.; Banerjee, D. Effects of silica nanoparticles on enhancing the specific heat capacity of carbonate salt eutectic (work in progress). *Int. J. Struct. Chang. Solids* **2010**, *2*, 25–31.
27. Shin, D.; Banerjee, D. Enhancement of specific heat capacity of high-temperature silica-nanofluids synthesized in alkali chloride salt eutectics for solar thermal-energy storage applications. *Int. J. Heat Mass Transf.* **2011**, *54*, 1064–1070.
28. Shin, D.H.; Banerjee, D. Enhanced specific heat of silica nanofluid. *J. Heat Transf.-Trans. Asme* **2011**, *133*, doi:10.1115/1.4002600.

29. Tiznobaik, H.; Shin, D. Enhanced specific heat capacity of high-temperature molten salt-based nanofluids. *Int. J. Heat Mass Transf.* **2013**, *57*, 542–548.
30. Tiznobaik, H.; Shin, D. Experimental validation of enhanced heat capacity of ionic liquid-based nanomaterial. *Appl. Phys. Lett.* **2013**, *102*, doi:10.1063/1.4801645.
31. Jo, B.; Banerjee, D. Enhanced specific heat capacity of molten salt-based nanomaterials: Effects of nanoparticle dispersion and solvent material. *Acta Mater.* **2014**, *75*, 80–91.
32. Chieruzzi, M.; Cerritelli, G.; Miliozzi, A.; Kenny, J. Effect of nanoparticles on heat capacity of nanofluids based on molten salts as PCM for thermal energy storage. *Nanoscale Res. Lett.* **2013**, *448*, doi:10.1186/1556-276X-8-448.
33. Andreu-Cabedo, P.; Mondragon, R.; Hernandez, L.; Martinez-Cuenca, R.; Cabedo, L.; Julia, J.E. Increment of specific heat capacity of solar salt with SiO₂ nanoparticles. *Nanoscale Res. Lett.* **2014**, *9*, 582.
34. Dudda, B.; Shin, D. Effect of nanoparticle dispersion on specific heat capacity of a binary nitrate salt eutectic for concentrated solar power applications. *Int. J. Therm. Sci.* **2013**, *69*, 37–42.
35. Tan, Z.C.; Wang, L.; Shi, Q. Study of heat capacity enhancement in some nanostructured materials. *Pure Appl. Chem.* **2009**, *81*, 1871–1880.
36. Oh, S.H.; Kauffmann, Y.; Scheu, C.; Kaplan, W.D.; Ruhle, M. Ordered liquid aluminum at the interface with sapphire. *Science* **2005**, *310*, 661–663.
37. Wang, L.; Tan, Z.C.; Meng, S.G.; Liang, D.B.; Li, G.G. Enhancement of molar heat capacity of nanostructured Al₂O₃. *J. Nanoparticle Res.* **2001**, *3*, 483–487.

© 2015 by the authors; licensee MDPI, Basel, Switzerland. This article is an open access article distributed under the terms and conditions of the Creative Commons Attribution license (<http://creativecommons.org/licenses/by/4.0/>).